

Effect of coarse aggregate quantity on fracture toughness of concretes

G. PROKOPSKI

Civil Engineering Department, Technical University of Czestochowa, Armii Krajowej 27, 42-200 Czestochowa, Poland

The results of fracture toughness tests performed according to mode II of loading for basalt and limestone concretes of different aggregate contents are presented. The stress intensity factor K_{IIC} was determined. The fractographical and microscopic studies were performed in an attempt to relate the parameters of concrete structure to its fracture toughness.

1. Introduction

The strength of concrete is strongly related to the phenomenon of primary fissures propagation, always present in the concrete bulk as a result of concrete setting. Inevitable defects and non-homogeneities occurring in the concrete structure produce stress concentrations. In the region of the highest stress concentration the nucleation of cracks leads to their propagation and, consequently, to failure. The fractographical analysis of materials of cement matrices performed on the basis of criteria describing the development and propagation of cracks is more reasonable than the use of data obtained in compression tests. The fracture of concrete does not occur as a result of exceeding the value of mean stresses (obtained in the compression test), but from reaching a sufficient level of energy in the region of the highest stress concentration (the longest or sharpest fissure) to cause crack propagation and lead to element failure.

In analysing the phenomena accompanying failure of materials with a cement matrix, the relation between its structure and strength, in terms of fracture toughness, is one of the most important factors. Recently, attempts to describe the phenomena accompanying the process of failure of cement-based materials in terms of their internal structure, although scarce, have been undertaken [1-3].

The results presented in these works concern the effect of coarse aggregate size [1], type of aggregate [2] and water/cement ratio on the process of micro-cracking of concrete [3].

As shown in the investigations of Stroeven [4], the strength of polyphase materials depends on the properties of individual phases and their percent volume fraction in the material bulk and structure, i.e. interaction and spatial configuration of phases.

One significant factor affecting the strength of concretes, although only recognized to a small extent, is the quantity of coarse aggregate in the concrete structure. In the literature one may find numerous concepts concerning the role of coarse aggregate and its effect on concrete strength. In the work by Mindess [5] it is stated that, in an ordinary concrete in which the

aggregate is stronger than the mortar, an increase in aggregate quantity causes an increase in the stress intensity factor, K_{Ic} . Naus and Lott [6] have given evidence that a distinct increase of K_{Ic} occurs as a result of an increase in quantity and diameter of coarse aggregate in the concrete structure. In the study by Bochenek and Prokopski [1] a distinct relationship between the diameter of coarse aggregate grains and the values of the stress intensity factor K_{IIC} and fracture energy J_{IIC} was shown. With an increase in diameter of gravel grains used for preparation of samples for the tests under mode II loading, an increase of both parameters tested, i.e. K_{IIC} and J_{IIC} , occurred, with a more distinct relationship in the case of J_{IIC} .

2. Experimental procedure

In this paper an attempt is made to establish the influence of quantity of basalt and limestone coarse aggregate on the fracture toughness of ordinary concrete with regard to the mechanism of cracking.

The individual concrete mixes containing both types of aggregates differed in quantity of coarse aggregate. The concretes contained the following weight proportion (cement:sand:coarse aggregate:water): basalt concrete—1:2.15:3.53:0.54; limestone concrete—1:2.16:3.56:0.56. However, two other mixes of basalt concrete were made where the quantities of coarse aggregate were increased and decreased by 10%. The other two mixes of limestone concrete were made with increased and decreased content of coarse aggregate, by 20 wt%. The cement was ordinary cement, the fine aggregate was from a local deposit and the coarse aggregate grains were 2-10 mm in diameter.

The following investigations have been carried out:

- (a) tests of the stress intensity factor K_{IIC} (mode II shearing);
- (b) fractographical tests using a Quantimet 720 image analyser;
- (c) microscopic tests using a Cambridge Scientific S4-10 electron microscope.

The compressive strength of concretes was tested with the use of 5 cubes (of side = 0.15 m), whereas the examination of fracture toughness was performed on 7 cubes (of side = 0.15 m) having two notches (Fig. 1).

The samples were cured for 7 days in a water bath and then stored under normal laboratory conditions for 21 days. After the 28 day curing period they were subjected to fracture toughness tests.

The strengths of concretes after pressure testing are shown in Table I.

2.1. Fracture toughness test

The tests of mode II fracture toughness was carried out on the stand presented in Fig. 2. The stress intensity factor K_{IIc} was determined according to a formula of Watkins [7]:

$$K_{IIc} = \frac{5.11 P_Q}{2BW} (\pi a)^{\frac{1}{2}} \quad (1)$$

where P_Q is the force initiating cracking (growth), which is identified in graphs as a minor deflection or extremum of the curve; B is the thickness under the crack; W is the height and a is the length of the crack. Table II contains values for the stress intensity factor, K_{IIc} , for both concretes, characterized by an individual basalt and limestone coarse aggregate quantity. The load-crack displacement curve was obtained for each specimen. Some specimen curves are shown in Fig. 3. In Fig. 4 the stress intensity factor K_{IIc} is plotted

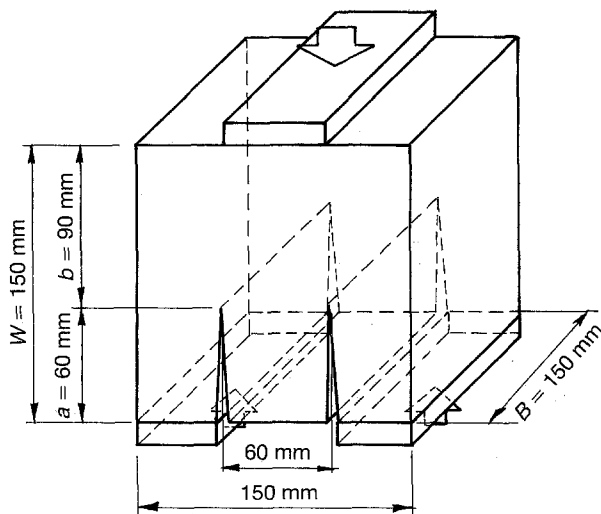


Figure 1 Test sample.

TABLE I The strength of concretes after pressure test.

	Basalt concrete		
	-	0	+
Strength after pressure test R [MPa] ± standard deviation	33.5 ± 6.6	34.1 ± 2.4	40.2 ± 4.7
	Limestone concrete		
	-	0	+
	32.2 ± 1.1	30.8 ± 0.6	31.9 ± 0.4

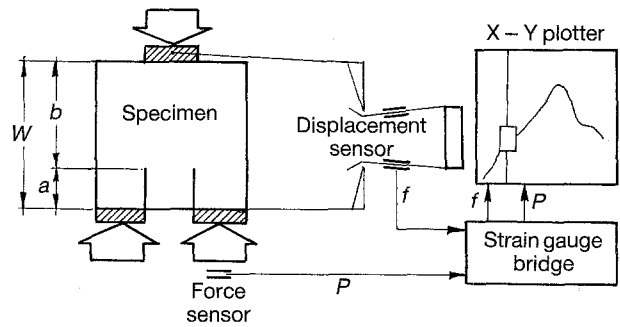


Figure 2 Scheme of test stand.

TABLE II Stress intensity factor K_{IIc}

	-	0	+
<u>Basalt concrete</u>			
K_{IIc} [MN m ^{-3/2}]	3.598	3.623	3.780
	4.856	3.665	4.067
	5.029	4.807	4.314
	5.119	5.423	4.806
	5.177	6.409	5.505
	5.546	6.623	5.735
	6.491	7.149	5.744
\bar{K}_{IIc}	5.116	5.308	4.850
± σ	0.862	2.375	0.823
<u>Limestone concrete</u>			
K_{IIc} [MN m ^{-3/2}]	2.670	2.876	3.081
	3.163	3.328	3.615
	3.656	3.369	3.821
	3.670	3.492	4.026
	3.697	4.232	4.273
	4.642	4.766	4.601
			5.546
\bar{K}_{IIc}	3.595	3.677	4.137
± σ	0.542	0.568	0.578

against basalt and limestone coarse aggregate quantity.

2.2. Fractographical tests

The quantitative description of fracture morphology of sample fracture surfaces obtained in fracture toughness tests was performed on the basis of analysis of profile lines.

The studies were performed with the use of a Quantimet 720 image analyser. The specimens subjected to this analysis were selected randomly from batches of samples made of basalt and limestone concretes with different quantities of coarse aggregate. The replicas were obtained by covering fracture surfaces with a hardening metacrylate resin. The replicas were cut into pieces, perpendicular to the fracture surface being mapped. 20 individual layers were obtained from each replica, enabling the examination of 40 profile lines (Fig. 5).

Linear roughness was also examined, $R_L = L'/L$; where L' is the actual length of the profile line and L is the projected length of the profile. The results of linear roughness R_L and the values of stress intensity factor K_{IIc} are presented in Table III.

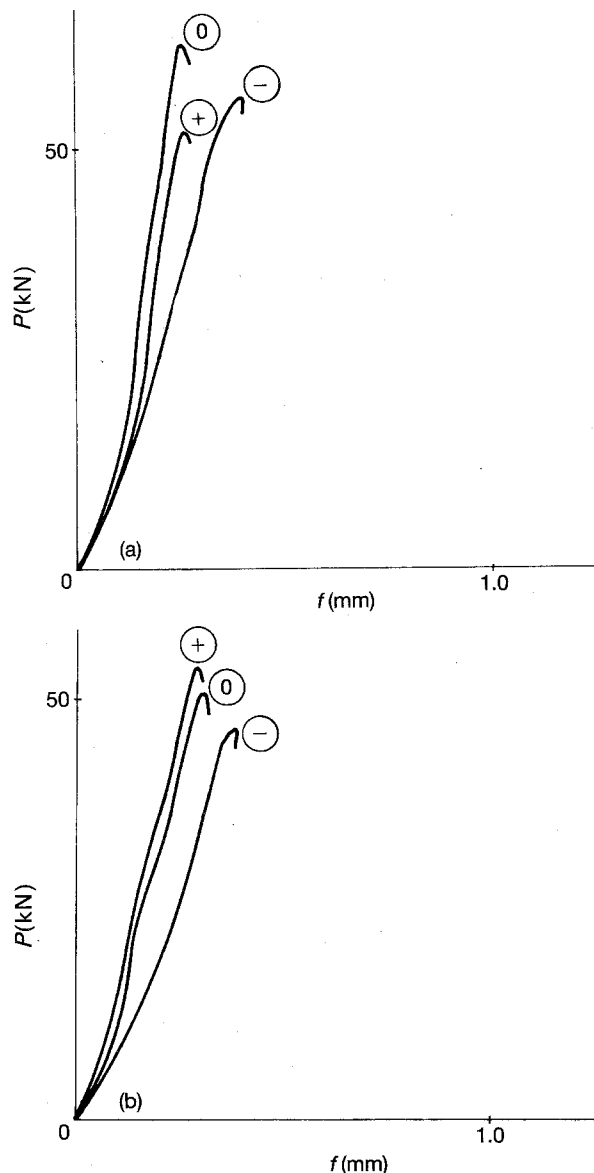


Figure 3 Exemplary load-displacement curves: (a) basalt concrete; (b) limestone concrete. - decreased quantity of coarse aggregate; 0 a basic quantity of coarse aggregate; + increased quantity of coarse aggregate.

TABLE III Results of profile lines investigations

Material tested	K_{IIc} [MN m ^{-3/2}]	R_L
Basalt concrete		
-	5.119	1.156
0	6.623	1.163
+	4.806	1.153
Limestone concrete		
-	4.642	1.109
0	4.766	1.112
+	4.030	1.105

2.3. Mechanism of microfracture

The tests were performed with the use of an S4-10 Cambridge Scientific SEM at a magnification of $\times 1000$. The studies have shown significant differences in the microstructures of concretes after fracture toughness tests.

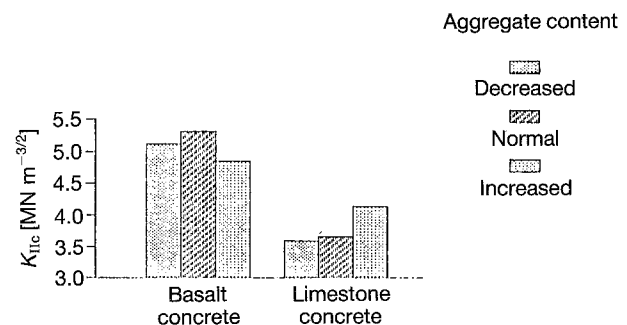
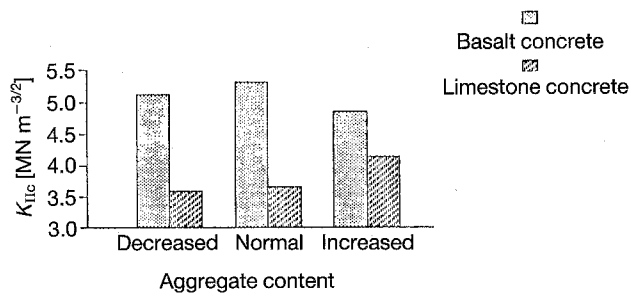


Figure 4 Stress intensity factor K_{IIc} .

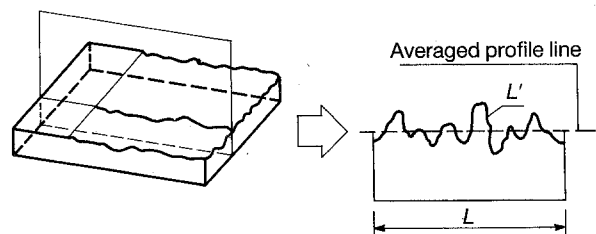


Figure 5 Method of preparing profile lines for tests.

In basalt concrete the cracks propagated along the basalt grains/cement paste interface and through the cement paste (Fig. 6). However, it was also possible to observe cleavage fracture of basalt grains (Fig. 7).

In the case of concrete with limestone aggregate the chemical reactivity and highly developed external surface of the grains resulted in very strong bonding between the cement paste and the limestone grains. In this concrete an aggregate/cement paste interface layer strongly attached to aggregate grains was observed. The cracks appeared at a certain distance from the aggregate grain/cement paste interface (*ca* 5–8 μm) (Fig. 8). Cracks propagating through the cement paste and arrested on the limestone aggregate were also observed (Fig. 9).

3. Discussion

The results of K_{IIc} studies obtained for both types of concretes confirm a significant effect of quantity and type of coarse aggregate on the values of this parameter.

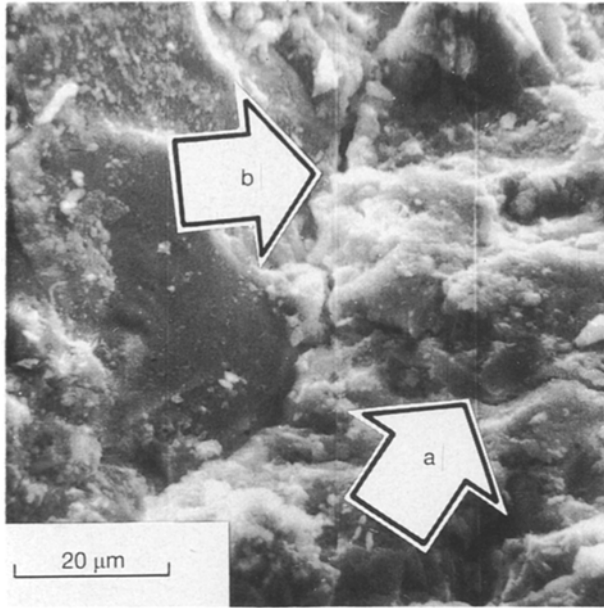


Figure 6 Microfracture of the basalt concrete. Microfractures across the cement paste and at the borderline between basalt grains and the cement paste are designated by a and b, respectively. Magnification $\times 1000$.

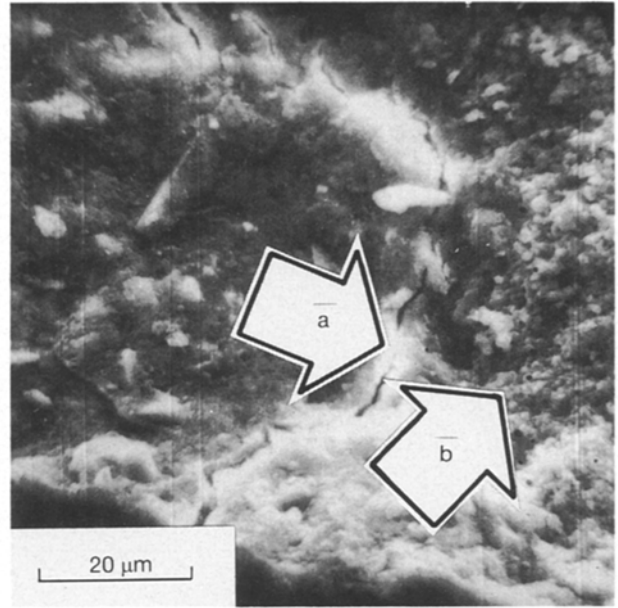


Figure 8 Microstructure of the limestone concrete. The contact layer between limestone grains and the cement paste are denoted as a and the characteristically developed surface of the limestone aggregate grain is denoted as b. Magnification $\times 1000$.

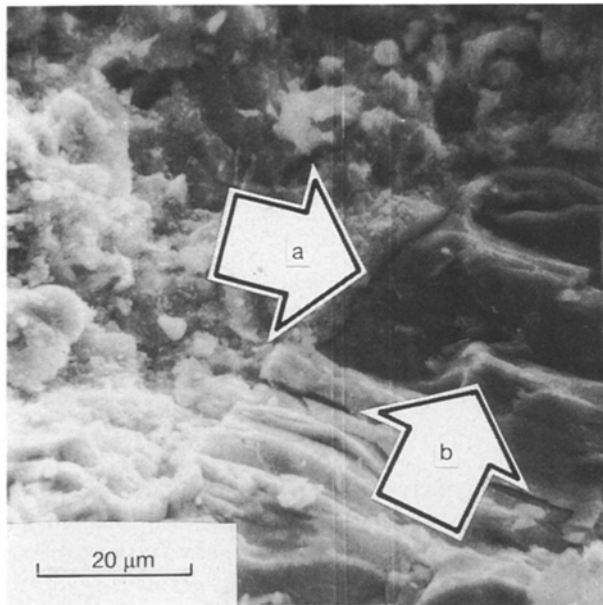


Figure 7 Microstructure of the basalt concrete. Terraced cleavage microfractures across a basalt grain and along the borderline between basalt grains and the cement paste are designated by a and b, respectively. Magnification $\times 1000$.

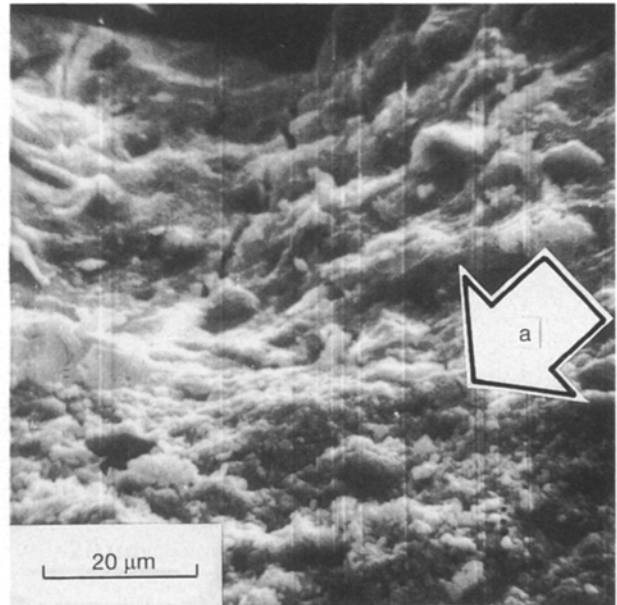


Figure 9 Microstructure of the limestone concrete. A microfracture running across the cement paste is denoted by a, impinging against the contact cement paste and a limestone grain. Magnification $\times 1000$.

The stronger basalt aggregate is chemically inactive, with the result that bonding forces on the aggregate grain/cement paste interface are relatively lower than in the case of concrete made of chemically active limestone aggregate. In the case of basalt concrete, the mechanical properties were dependent on the properties of the aggregate, whereas the strength of limestone concrete was more closely related to the values of aggregate/cement paste bonding forces.

The examination of the linear roughness of profile line R_L has shown the existence of a relationship between fracture surface morphology and stress

intensity factor K_{IIc} . The fracture surface character depends on the strength of coarse aggregate grains and on the cohesive forces between aggregate grains and cement paste, as well as on the shape morphology of coarse aggregate grains. Interrelations that take place between these factors in particular concretes determine the amount of energy necessary for sample failure and influence the character of fracture surfaces forming during the failure. Analysis of the micrographs showed that the reactivity and the highly developed surface of the limestone aggregate grains generate high cohesive forces on the aggregate/cement

paste interface. The cohesive forces in this case were higher than the strength of the cement paste itself. This resulted in the cracks appearing outside the grain/cement paste interface. In the case of basalt concrete the cracks appeared on the basalt grains/cement paste interface or nucleated and propagated in the cement paste.

References

1. A. BOCHENEK and G. PROKOPSKI, *Int. J. Fracture* **41** (1989) 197.
2. *Idem.*, *Archiwum Inżynierii Lądowej* **35** (1989) 49 (in Polish).

3. G. PROKOPSKI, *J. Mater. Sci.* **26** (1991) 6352.
4. P. STROEVEN, PhD Thesis, Technological Universitet of Delft (1973).
5. S. MINDESS, in "Mechanika Kompozytów Betonopodobnych (Ossolineum, Wrocław, 1983) p. 377 (in Polish).
6. D. J. NAUS and J. L. LOTT, *J. Amer. Concrete Inst.* **6** (1969) 481.
7. J. WATKINS, *Int. J. Fracture* **23** (1983) R135.

Received 1 May 1992

and accepted 24 February 1993